Strong jet and a new thermal wave in Saturn's equatorial stratosphere

Li Liming,[1] Peter J. Gierasch,[1] Richard K. Achterberg,[2] Barney J. Conrath,[1]
F. Michael Flasar,[3] Ashwin R. Vasavada,[4] Andrew P. Ingersoll,[5] Don Banfield,[1]
Amy A. Simon-Miller,[3] and Leigh N. Fletcher[4]

[1]   The strong jet, with a speed between 500 and 600 m/s, is inferred in the equatorial region of Saturn by combining the nadir and limb observations of Composite Infrared Spectrometer (CIRS) aboard the Cassini spacecraft. A similar jet was discovered on Jupiter (F. M. Flasar et al., 2004a). These discoveries raise the possibility that intense jets are common in the equatorial stratospheres of giant planets. An equatorial wave with wavenumber ~9 is revealed in the stratosphere of Saturn by the CIRS high spatial-resolution thermal maps. Our discussion based on the phase velocity suggests that the equatorial wave is probably a Rossby-gravity wave. The discovery of an equatorial wave in the stratosphere suggests that Saturn's equatorial oscillations (T. Fouchet et al., 2008; G. S. Orton et al., 2008) may be driven by vertically propagating waves, the same mechanism that drives the quasi-biennial oscillation (QBO) on Earth.
Citation: Liming, L., P. J. Gierasch, R. K. Achterberg, B. J. Conrath, F. M. Flasar, A. R. Vasavada, A. P. Ingersoll, D. Banfield, A. A. Simon-Miller, and L. N. Fletcher (2008), Strong jet and a new thermal wave in Saturn's equatorial stratosphere, *Geophys. Res. Lett.*, *35*, L23208, doi:10.1029/2008GL035515.

1.   Introduction

[2]   The intense equatorial jets on giant planets are among the amazing phenomena in our solar system. Unlike its more stable counterpart on Jupiter [*Porco et al.*, 2003; *Li et al.*, 2004], Saturn's equatorial jet displays some variability. Cloud tracking studies on HST images between 1995 and 2002 suggests a weaker equatorial jet on Saturn than that measured by Voyager between 1981 and 1982 [*Sanchez-Lavega et al.*, 2003]. However, the multi-spectral images from Cassini's Imaging Science Subsystem (ISS) indicate that the apparent slowing of the equatorial jet on Saturn from the Voyager epoch to the HST epoch can be partly explained if the observed tracers occurred at different altitudes within a jet with vertical shear in the horizontal velocity [*Porco et al.*, 2005]. The observations from Cassini's Composite Infrared Spectrometer (CIRS) seem to support the ISS interpreta-

tion by showing that zonal winds decrease with altitude at ~10°S [*Flasar et al.*, 2005]. Three recent studies imply that Saturn's equatorial jet varies with both altitude and time [*Perez-Hoyos and Sanchez-Lavega*, 2006; *Sayanagi and Showman*, 2007; *Sanchez-Lavega et al.*, 2007]. Obviously, a detailed study of the vertical structure and the time variation of the equatorial jet on Saturn will help to clarify the above debate.

[3]   Analogous to the equatorial oscillations in Earth's atmosphere [*Baldwin et al.*, 2001] and Jupiter [*Leovy et al.*, 1991; *Friedson*, 1999; *Simon-Miller et al.*, 2007], semi-annual oscillations (SAO) are discovered in the equatorial region of Saturn [*Fouchet et al.*, 2008; *Orton et al.*, 2008]. The discovery of SAO on Saturn raises the possibility that quasi-periodic oscillations are a common phenomenon in planetary stratospheres. However, the physics behind the SAO on Saturn is unclear. The vertical propagation of waves plays an important role in the equatorial oscillations of Earth and Jupiter [*Lindzen and Holton*, 1968; *Friedson*, 1999]. A related question has to be asked: do waves play an important role in the equatorial oscillation on Saturn?

[4]   The Composite Infrared Spectrometer (CIRS) aboard Cassini acquired high-spatial-resolution nadir scans of Saturn's global atmosphere from 2004 to 2008, which offer a perfect opportunity to examine the equatorial region of Saturn. These observations were utilized to create the zonal-mean temperatures [*Fletcher et al.*, 2007] and the thermal maps of the polar regions of Saturn [*Fletcher et al.*, 2008] in the previous studies. Here, we apply a modified thermal wind equation to the zonal-mean temperatures over 4 years (2004–2008) to explore the vertical structure of the equatorial jet on Saturn. In addition, the high-spatial-resolution thermal maps of the equatorial region, which was not covered in the previous study [*Fletcher et al.*, 2008], are utilized to search for the equatorial waves on Saturn.

2.   Data and Methodology

[5]   The Cassini/CIRS, a Fourier-transform Spectrometer described elsewhere [*Flasar et al.*, 2004b], is a critical instrument on Cassini to explore the thermal structure of a planetary atmosphere. The CIRS observed Saturn's northern and southern hemispheres from 2004 to 2008 so that a series of hemispheric maps are available, but the time separation between the neighboring two hemispheric maps is irregular, varying between half a day and a few months. Some of these observations scanned through the equator, capturing the equatorial region. In this study, we will mainly utilize the nadir observations in the mid-infrared band (600 cm^{-1}–1400 cm^{-1}) with a spectral resolution of 15 cm^{-1}. The nadir observations have the highest hori-

---

[1]Department of Astronomy, Cornell University, Ithaca, New York, USA.
[2]Department of Astronomy, University of Maryland, College Park, Maryland, USA.
[3]NASA Goddard Space Flight Center, Greenbelt, Maryland, USA.
[4]Jet Propulsion Laboratory, California Institute of Technology, Pasadena, California, USA.
[5]Division of Geological and Planetary Sciences, California Institute of Technology, Pasadena, California, USA.
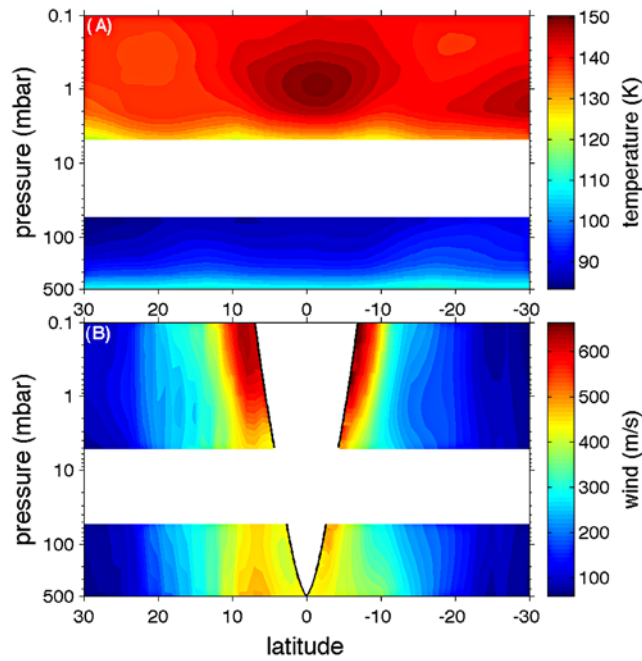
Figure 1. Zonal-mean CIRS temperatures and the corresponding thermal winds. (a) Temperatures averaged over ~4 years (October, 2004 to March, 2008). (b) Inferred zonal winds corresponding to Figure 1a based on the modified thermal wind equation. The combined zonal winds from Voyager and Cassini observations are used as a lower boundary condition at 500 mbar. The region within the black lines, which are the cylinders tangent to the equator at 500 mbar, are left blank because the modified thermal wind still does not work there. The region between 5 and 50 mbar has also been removed for the CIRS nadir observations have no spectral sensitivity there.

zontal spatial resolution, which is critical for using our modified thermal wind equation and examining wave patterns. The mid-infrared interferometer consists of two 1 x 10 arrays of 0.3-mrad pixels (FP3 and FP4). The focal plane FP3 includes a pressure-induced absorption band S(1) line of H_2, which can be utilized to retrieve the thermal structure between 50 mbar and 500 mbar [*Conrath et al.*, 1998; *Flasar et al.*, 2004b]. The other mid-infrared focal plane FP4 is designed to capture the CH_4 emission band around 1300 cm^{-1}, which can be utilized to retrieve the temperature in the stratosphere (0.5 mbar−5 mbar). The retrieval scheme of CIRS is a relatively mature inversion algorithm and described elsewhere [*Conrath et al.*, 1998]. We retrieve both upper tropospheric and stratospheric temperature maps with a spatial resolution of 1° in latitude and 2° in longitude from the CIRS high-spatial-resolution nadir radiance. The temperature maps retrieved from the CIRS nadir scans have much higher spatial resolution in the horizontal plane than those from the CIRS limb observations, making the former more useful for deriving the vertical structure of the equatorial jet using the thermal wind equation. In addition, the retrieved upper tropospheric and stratospheric temperatures make it possible to utilize the cloud-tracked winds as a lower boundary condition to estimate actual stratospheric wind speeds,

which is different from the previous study based on the limb observations [*Fouchet et al.*, 2008].

[6] The standard thermal wind equation, which relates the vertical wind shear to the horizontal temperature gradient along isobaric surfaces, can be used to derive the vertical structure of wind if the temperature field is known, or vice versa. However, the simple-format standard thermal wind equation stops working in the equatorial region because the geostrophic balance, which is one assumption behind the standard thermal wind equation, ceases to be valid when approaching the equator. More importantly, the large variation of large-scale jets, rotation periods, and radii of different planets means that some forces discarded in the geostrophic balance and the hydrostatic balance are not negligible [*Li et al.*, 2007]. We have examined a modified thermal wind equation [*Li et al.*, 2007], which is applicable to the low latitudes of planets. In the equatorial region, the modified thermal wind equation (please see auxiliary material[1]) is better than the standard thermal wind equation, which has already been used in a previous study [*Read et al.*, 2007]. The modified thermal wind equation can be expressed as

$$\frac{\partial}{\partial z}\Big|_{r_c}\left(\frac{u^2 + 2\Omega u r_c}{r_c}\right) = \frac{R}{pr}\frac{\partial p}{\partial r}\frac{\partial T}{\partial \phi}\Big|_p \qquad (1)$$

where z is an unit vector along the rotation axis, r_c is the cylindrical radius, u is the zonal wind, Ω is the angular speed of rotation of the planet, R is the specific gas constant, P is the pressure, r is the radius of planets, T is the temperature, and ϕ is the latitude.

[7] We integrated the above thermal wind equation along the cylinders parallel to the rotation axis with the CIRS high-spatial-resolution (1° in the latitudinal direction) thermal maps and the known 500-mbar zonal winds. The zonal winds at pressure level 500-mbar mainly come from the Voyager observations [*Ingersoll et al.*, 1984]. We interpolate the relatively low spatial-resolution winds (~2°) from the Voyager observations to the high-resolution zonal winds (1°) in order to use the high-spatial-resolution CIRS temperature fields. Also the gap between 1°S to 27°S in Voyager measurements is filled by the observations from Cassini ISS images [*Porco et al.*, 2005]. The combined zonal winds from Voyager and Cassini observations are relative to the rotation period of Saturn based on Voyager measurements [*Desch and Kaiser*, 1981]. The possible variations of the rotation period of Saturn [*Gurnett et al.*, 2005, 2007; *Anderson and Schubert*, 2007] are not considered in this study. The above thermal wind equation still cannot work for the region equator-ward and above the cylinders tangent to the equator at 500 mbar (black lines in Figure 1).

3. Results

[8] Figure 1 shows the zonal-mean CIRS temperatures and the corresponding zonal winds in the equatorial region of Saturn. The panel A of Figure 1 represents an average temperature structure over 4 years (2004−2008), which is
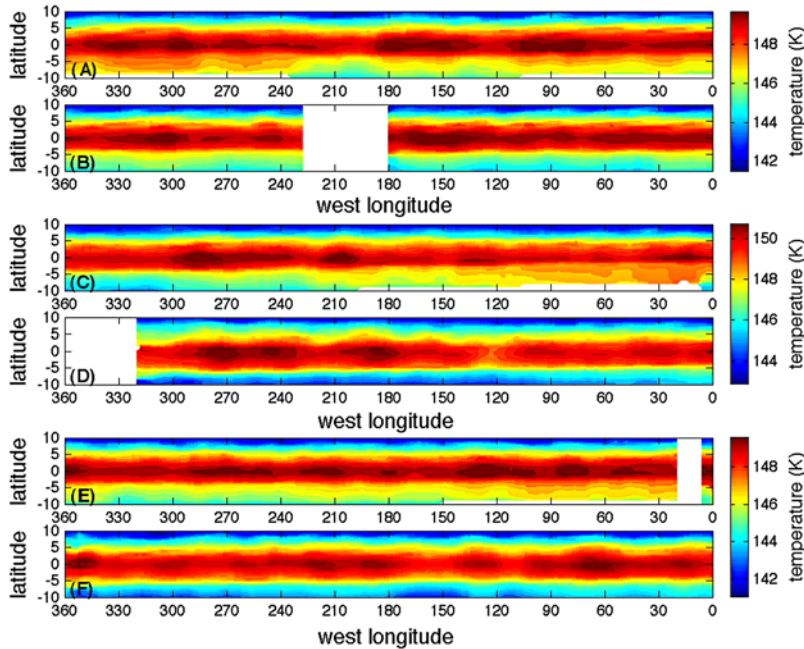
Figure 2. Time sequence of CIRS 1-mbar temperature maps with spatial resolution 1° and 2° in the latitudinal and longitudinal directions, respectively. (a) and (b) Two temperature maps observed in March 10−11, 2005, which are separated by 11 hours. (c) and (d) Two temperature maps observed in May 22−23, 2005, which are separated by 11 hours. (e) and (f) Two temperature maps observed in March 22−23, 2006, which are separated by 21 hours. The blank areas indicate gaps in data coverage.

basically consistent with the temperature structure over 18 months (2004−2006) in the previous study [*Fletcher et al.*, 2007]. The similarity between this study and the previous study suggests that the basic structures of the zonal-mean temperature in Saturn's equatorial region are relatively stable during 2004−2008, which is during the northern hemisphere's winter. The equatorial jet (panel B) displays a decrease of strength from the level of the tropospheric cloud deck (∼500 mbar) to the middle of stratosphere (∼1 mbar) between 7°S and 20°S in the southern hemisphere, which is consistent with the previous study [*Flasar et al.*, 2005]. Figure 1b further shows that the increase of zonal wind with altitude in the stratosphere results in a very strong jet (∼600 m/s at pressure levels around and above 1 mbar) in the equatorial region. The region between 5 and 50 mbar in Figure 1 is left blank because the CIRS nadir spectra have no spectral sensitivity there. The CIRS limb observations suggest a cold center around 10 mbar at the equator [*Fouchet et al.*, 2008]. This cold center results in a decrease of zonal wind by ∼100 m/s with altitude in that region by the thermal wind equation [*Fouchet et al.*, 2008], which will lessen the strength of our inferred equatorial jet in Saturn's stratosphere from ∼600 m/s to ∼500 m/s. The above discussion suggests that Saturn has an even stronger equatorial jet ∼500−600 m/s in the stratosphere than in the troposphere, making it the strongest atmospheric jet ever discovered in our solar system. The recent measurements from Cassini's Visual and Infrared Mapping Spectrometer (VIMS) [*Baines et al.*, 2005; D. S. Choi et al., Cloud features and zonal wind measurements of Saturn's atmosphere as observed by VIMS, submitted to *Journal of Geophysical Research*, 2008] suggests that Sat-

urn's equatorial jet can reaches speeds exceeding 450 m/s at the relatively deep atmosphere ∼1−2 bar. The observations from Cassini's multiple instruments (CIRS, ISS and VIMS) depict a basic picture for the vertical structure of equatorial jet on Saturn: The equatorial jet with speed ∼400−500 m/s at the upper troposphere (∼0.5−2 bar) decreases to ∼300−400 m/s around the tropopause (∼10−100 mbar), then it increases to ∼500−600 m/s in the middle stratosphere (∼1 mbar). Jupiter has the same vertical structure of equatorial jet [*Gierasch et al.*, 1986; *Flasar et al.*, 2004a], which implies such a configuration of equatorial jet is a common phenomenon for giant planets.

[9] The temperature field and the inferred wind field offer us an opportunity to check the stability of atmosphere on Saturn. Our estimate based on the temperature in Figure 1 shows that the Brunt-Vaisala (buoyancy) frequency (N^2) is on the order of 10^{-5} s^{-2}, which suggests that Saturn's atmosphere is convectively stable in the upper troposphere and the middle stratosphere. The estimates of wind shear (dU^2/dz^2) based on the thermal winds in Figure 1 and a simple scalar analysis show that the wind shear is less than the order of 10^{-7} s^{-2}. Therefore, the Richardson number Ri ($Ri = N^2/(dU^2/dz^2)$) is much larger than one, which suggests that the Kelvin-Helmholtz (KH) instability is suppressed in the upper troposphere and the middle stratosphere of Saturn.

[10] The high-spatial-resolution CIRS maps also make it possible to examine the existence of the equatorial waves on Saturn. The time sequence of temperature maps at 1 mbar is shown in Figure 2. The 1-mbar thermal maps display an obvious longitudinal wave between 5°S and 5°N. A periodogram analysis (Figure S1) suggests the equatorial wave

has a wavelength $\sim 40°$ in the longitudinal direction. The confidence level of the spectrum (>99%) suggests that the $40°$ wavelength in the longitudinal direction is fairly robust. The $40°$ wavelength is equivalent to a wavenumber of 9 around the globe.

[11] The cross-correlation of the equatorial wave between two pressure levels with maximal inversion kernel (1 mbar and 3 mbar) (Figure S2) does not show any noticeable shift in longitudinal direction, which suggests that the vertical wavelength of the stratospheric wave has a vertical wavelength longer than the distance between 1 mbar and 3 mbar (~ 1 scale height, H). The 100-mbar temperature maps do not show the equatorial wave with wave-number 9. In addition, the multi-filter images from the Cassini Imaging Science Subsystem (ISS) (Figure S3) with effective pressure levels deeper than 100 mbar also imply that the equatorial wave in the stratosphere does not propagate downward to 100 mbar. The above discussions suggest that vertical wavelength of the equatorial wave in the stratosphere is shorter than the distance between 1 mbar and 100 mbar, or $\sim 4.5H$. In summary, the vertical wavelength L_z has a range of $1H-4.5H$.

[12] The two pairs separated by 11 hours in Figures 2a, 2b, 2c, and 2d display noticeable westward movement for the 1-mbar equatorial wave. The cross-correlation between the temperature maps separated by 11 hours (Figure S4) has a maximum of ~ 0.6 at the equator when the longitudinal shift is $18°$, corresponding to a phase velocity $C_x \sim 470$ m/s in the longitudinal direction. A linear interpolation from the two sides of the equator (Figure 1b) suggests that the zonal wind around the equator at ~ 1 mbar is about 600 m/s. The phase velocity of equatorial wave in stratosphere is smaller than the background zonal wind. The comparison between the phase velocity C_x and the background zonal wind u suggests that the equatorial wave in the stratosphere moves westward with a velocity ~ 130 m/s relative to background zonal current ($C_x - u = -130$ m/s). If we take the possible decrease of ~ 100 m/s around 10 mbar from Cassini limb observations [*Fouchet et al.*, 2008] into account, the equatorial wave in the stratosphere still moves westward with a velocity ~ 30 m/s relative to the strong background current ($C_x - u = -30$ m/s). It should be emphasized that the range (500 m/s$-$600 m/s) of the background current around the equator at ~ 1 mbar has uncertainties associated with the retrieved temperature, the zonal wind at the lower boundary and its pressure level, the modified thermal wind equation itself, and the interpolation from the two sides of the equator. It is possible that the combined uncertainty in the background current changes the moving direction of the equatorial wave relative to the background current.

[13] Small-scale gravity waves, whose wavelength is shorter than ~ 100 km, are still cannot resolved by the high-spatial-resolution CIRS thermal maps with a spatial resolution of $1°$ in latitude (~ 1000 km at the equator) and $2°$ in longitude (~ 2000 km at the equator). There are two kinds of planetary-scale equatorial waves that satisfy the condition of quick decay away from the equator: Rossby-gravity waves and Kelvin waves. The equatorial Rossby-gravity wave must propagate westward relative to the background current ($C_x - u < 0$) and the equatorial Kelvin wave must propagate eastward relative to the background current ($C_x - u > 0$) if they are trapped in the equatorial

region [*Holton*, 2004]. The phase velocity of the equatorial Rossby-gravity wave can be expressed as [*Holton*, 2004]

$$C_x - u = \sqrt{gh_e} \left[\frac{1}{2} - \frac{1}{2} \left(1 + \frac{4\beta}{k_x^2 \sqrt{gh_e}} \right)^{1/2} \right] \quad (2)$$

where k_x is the wave-number in the longitudinal direction, β is the variation of Coriolis parameter with the latitude, and gh_e is the production of gravity g and mean depth of background atmosphere h_e, which can be expressed as $gh_e = N^2/(k_z^2 + 1/4H^2)$ with the vertical wave-number k_z. The parameter β at the equator is $\beta = 2\Omega/r = 5.63 \times 10^{-12}$ s^{-1} m^{-1}. The longitudinal wavelength of the equatorial wave is $\sim 40°$, which suggests the wave-length and wave-number in the longitudinal direction as $L_x = r \times 40 \times \pi/180 = 4.12 \times 10^7$ m and $k_x = 2\pi/L_x = 1.53 \times 10^{-7}$ m^{-1}, respectively. The scale height has the value of $H = RT/g = 5.8 \times 10^4$ m at 1-mbar. The vertical wave-length has the range of $H < L_z < 4.5H$, which implies that the vertical wave-number has the range of 5.80×10^{-10} m$^{-2} < k_z^2 < 1.17 \times 10^{-8}$ m^{-2}. Based on the CIRS retrieved temperatures, the Brunt-Vaisala (buoyancy) frequency N^2 at 1-mbar can be estimated as $N^2 = g(g/C_p - \partial T/\partial z)/T \sim 5.8 \times 10^{-5}$ s^{-2}. Substituting the above parameters into equation (2), we have -150 m/s $< C_x - u < -90$ m/s, which is barely consistent with our previous estimate (-130 m/s $< C_x - u < -30$ m/s). Likewise, we can estimate the phase velocity of the equatorial Kelvin wave relative to the background current have the range as 250 m/s $< C_x - u = \sqrt{gh_e} <$ 950 m/s, which is far from our previous estimate. Therefore, we think that the equatorial wave is probably a Rossby-gravity wave.

[14] The planetary-scale Rossby-gravity wave contributes to the westward stresses of the equatorial oscillations, whereas planetary-scale Kelvin wave contributes to the eastward stresses of the equatorial oscillations [*Wallace*, 1973]. The latter has not been observed in the equatorial region of Saturn. Small-scale gravity waves, which contribute to both the eastward and westward stresses of the equatorial oscillations [*Lindzen and Holton*, 1968; *Friedson*, 1999], are not resolved in our current observations either. However, the westward propagating Rossby-gravity wave discovered in Saturn's equatorial stratosphere suggests that the wave-driving theory behind the equatorial oscillations on Earth and Jupiter is probably applicable to Saturn.

4. Conclusions

[15] The Cassini/CIRS high-spatial-resolution nadir observations are utilized to examine the equatorial region of Saturn with the emphasis to the jet and wave activities. A relatively complete picture of the equatorial jet is obtained by combining the CIRS high-spatial-resolution temperature field and the modified thermal wind equation. In addition, a new thermal wave is discovered in the equatorial region, which is possibly related to the equatorial oscillations on Saturn.

[16] A long-term comparison of the temperature field and the related thermal winds between the Voyager epoch and the Cassini epoch will shed more light on the equatorial region of Saturn. Theoretical models of the propagation of

equatorial waves and their roles in the equatorial oscillations [*Achterberg and Flasar*, 1996; *Friedson*, 1999] are also proposed.

References

Achterberg, R. K., and F. M. Flasar (1996), Planetary-scale thermal waves in Saturn's upper troposphere, *Icarus*, *119*, 350–369.

Anderson, J. D., and G. Schubert (2007), Saturn's gravitational field, internal rotation, and interior structure, *Science*, *317*, 1384–1387.

Baines, K. H., T. W. Momary, and M. Roos-Serote (2005), The deep winds of Saturn: First measurements of the zonal wind field near the two-bar level, *Bull. Am. Astron. Soc.*, *37*, 658.

Baldwin, M. P., et al. (2001), The quasi-biennial oscillation, *Rev. Geophys.*, *39*, 179–229.

Conrath, B. J., P. J. Gierasch, and E. A. Ustinov (1998), Thermal structure and para hydrogen fraction on the outer planets from Voyager IRIS measurements, *Icarus*, *135*, 501–517.

Desch, M. D., and M. L. Kaiser (1981), Voyager measurement of the rotation period of Saturn's magnetic-field, *Geophys. Res. Lett.*, *8*, 253–256.

Flasar, F. M., et al. (2004a), An intense stratospheric jet on Jupiter, *Nature*, *427*, 132–135.

Flasar, F. M., et al. (2004b), Exploring the Saturn system in the thermal infrared: The Composite Infrared Spectrometer, *Space Sci. Rev.*, *115*, 169–297.

Flasar, F. M., et al. (2005), Temperatures, winds, and composition in the Saturnian system, *Science*, *307*, 1247–1251.

Fletcher, L. N., P. G. J. Irwin, N. A. Teanby, G. S. Orton, P. D. Parrish, R. de Kok, C. Howett, S. B. Calcutt, N. Bowles, and F. W. Taylor (2007), Characterising Saturn's vertical temperature structure from Cassini/CIRS, *Icarus*, *189*, 457–478.

Fletcher, L. N., et al. (2008), Temperature and composition of Saturn's polar hot spots and hexagon, *Science*, *319*, 79–81.

Fouchet, T., S. Guerlet, D. F. Strobel, A. A. Simon-Miller, B. Bezard, and F. M. Flasar (2008), An equatorial oscillation in Saturn's middle atmosphere, *Nature*, *453*, 200–202.

Friedson, A. J. (1999), New observations and modeling of a QBO-like oscillation in Jupiter's stratosphere, *Icarus*, *137*, 34–55.

Gierasch, P. J., B. J. Conrath, and J. A. Magalhaes (1986), Zonal mean properties of Jupiter upper troposphere from Voyager infrared observations, *Icarus*, *67*, 456–483.

Gurnett, D. A., et al. (2005), Radio plasma wave observations at Saturn from Cassini's approach and first orbit, *Science*, *307*, 1255–1259.

Gurnett, D. A., A. M. Persoon, W. S. Kurth, J. B. Groene, T. F. Averkamp, M. K. Dougherty, and D. J. Southwood (2007), The variable rotation period of the inner region of Saturn's plasma disk, *Science*, *316*, 442–445.

Holton, J. R. (2004), *An Introduction to Dynamic Meteorology*, 4th ed., Academic, San Diego, Calif.

Ingersoll, A. P., R. F. Beebe, B. J. Conrath, and G. E. Hunt (1984), Structure and dynamics of Saturn's atmosphere, in *Saturn*, edited by T. Gehrels and M. S. Matthews, Univ. of Arizona Press, Tucson.

Leovy, C. B., A. J. Friedson, and G. S. Orton (1991), The quasiquadrennial oscillation of Jupiter's equatorial stratosphere, *Nature*, *354*, 380–382.

Li, L., A. P. Ingersoll, A. R. Vasavada, C. C. Porco, A. D. Del Genio, and S. P. Ewald (2004), Life cycles of spots on Jupiter from Cassini images, *Icarus*, *172*, 9–23.

Lindzen, R. S., and J. R. Holton (1968), A theory of quasi-biennial oscillation, *J. Atmos. Sci.*, *25*, 1095–1107.

Orton, G. S., et al. (2008), Semi-annual oscillations in Saturn's low-latitude stratospheric temperatures, *Nature*, *453*, 196–199.

Perez-Hoyos, S., and A. Sanchez-Lavega (2006), On the vertical wind shear of Saturn's equatorial jet at cloud level, *Icarus*, *180*, 161–175.

Porco, C. C., et al. (2003), Cassini imaging of Jupiter's atmosphere, satellites, and rings, *Science*, *299*, 1541–1547.

Porco, C. C., et al. (2005), Cassini imaging science: Initial results on Saturn's atmosphere, *Science*, *307*, 1243–1247.

Read, P. L., L. N. Fletcher, P. G. J. Irwin, J. G. Barney, and R. Achterberg (2007), Zonal mean dynamics on Saturn from Cassini and Voyager data, *Bull. Am. Astron. Soc.*, *39*, 487.

Sanchez-Lavega, A., S. Perez-Hoyos, J. F. Rojas, and R. G. French (2003), A strong decrease in Saturn's equatorial jet at cloud level, *Nature*, *423*, 623–625.

Sanchez-Lavega, A., R. Hueso, and S. Perez-Hoyos (2007), The three-dimensional structure of Saturn's equatorial jet at cloud level, *Icarus*, *187*, 510–519.

Sayanagi, K. M., and A. P. Showman (2007), Effects of a large convective storm on Saturn's equatorial jet, *Icarus*, *187*, 520–539.

Simon-Miller, A. A., B. W. Poston, G. S. Orton, and B. Fisher (2007), Wind variations in Jupiter's equatorial atmosphere: A QQO counterpart?, *Icarus*, *186*, 192–203.

Wallace, J. M. (1973), General circulation of tropical lower stratosphere, *Rev.Geophys.*, *11*, 191–222.

———————————

R. K. Achterberg, Department of Astronomy, University of Maryland, College Park, MD 20742, USA.

D. Banfield, B. J. Conrath, P. J. Gierasch, and L. Liming, Department of Astronomy, Cornell University, Ithaca, NY 14853, USA. (liming@astro.cornell.edu)

F. M. Flasar and A. A. Simon-Miller, NASA Goddard Space Flight Center, Greenbelt, MD 20771, USA.

L. N. Fletcher and A. R. Vasavada, Jet Propulsion Laboratory, California Institute of Technology, Pasadena, CA 91109, USA.

A. P. Ingersoll, Division of Geological and Planetary Sciences, California Institute of Technology, Pasadena, CA 91125, USA.